Human Pose Recovery for Rehabilitation Using Ambulatory Sensors

Jonathan Feng-Shun Lin and Dana Kulić

Abstract— **In this paper, an approach for lower-leg pose recovery from ambulatory sensors is implemented and validated in a clinical setting. Inertial measurement units are attached to patients undergoing physiotherapy. The sensor data is combined with a kinematic model within an extended Kalman filter framework to perform joint angle estimation. Anthropometric joint limits and process noise adaptation are employed to improve the quality of the joint angle estimation. The proposed approach is tested on 7 patients following total hip or knee joint replacement surgery. The proposed approach achieves an average root-mean-square error of 0.12 radians at key poses.**

I. INTRODUCTION

The estimation of human posture during movement is an important research field with numerous applications, such as rehabilitation, human-machine interaction, physiotherapy and sports training. During rehabilitation, the physiotherapist assesses the patient's current status, then assigns a set of exercises to improve the patient's range of motion, strength and balance. Goniometry, a technique for the measurement of body joint angles, is commonly employed in the physiotherapy clinic, but can only be utilized when the patient is stationary. A system that can determine joint angles while the patient is in motion would provide the physiotherapist with relevant information throughout the rehabilitation session.

A system for estimating human joint angles can be realized by employing inertial measurement units (IMUs), typically consisting of accelerometers and gyroscopes, to collect movement data from the patient. IMU systems are a popular choice for joint angle recovery systems as they are cheap, small and do not require line of sight or have any other environmental requirements [1]. This makes IMUs a suitable choice for physiotherapy clinics, where patients and therapists are frequently moving around in the collection space. These movements occlude line of sight, making it difficult to employ technologies such as cameras.

Many existing works take advantage of IMUs to determine joint angles [2], [3], [4], [5]. A simple approach is to use accelerometers as inclinometers [2]. However, if the subject's acceleration is comparable to gravity, it becomes difficult to differentiate between the acceleration caused by the subject's inertial movements and the acceleration from gravity, decreasing the accuracy of the inclinometer. Systems combining accelerometers and gyroscopes within a complementary filter [3] have also been developed. Gyroscopes provide an accurate measurement of inertial movement, but imperfect gyroscope calibrations can produce a non-zero angular velocity measurement when no motion is actually occurring. This offset causes drift after integration, resulting in divergence of the orientation estimate. These errors can be reduced by employing more powerful filters such as the Kalman filter [4], which provide a more systematic method to fuse sensor measurements. The accuracy of the Kalman filter can be improved with the inclusion of a model of the articulated kinematic chain [5]. To further reduce drift, anthropometric joint limits are enforced by a potential field, and the process noise adjusted on-line [5].

However, the algorithms described above have only been verified on healthy subjects. Healthy subjects exhibit smooth and consistent motion, with a high degree of repeatability and little variance between repetitions. These motion characteristics may not be the same for rehabilitation patients, due to increased impairment from injury or surgery. In addition, rehabilitation patients tend to be older, and may suffer from degenerative conditions that could introduce tremors. These factors combine to increase noise, and could lead to increased difficulties in joint angle estimation.

While clinical testing has been undertaken with other automated rehabilitation tools, such as rehabilitation robots [6], [7], [8] and IMU systems for the analysis of gait [9], [10], specific assessment exercises [11], or fall detection [12], to the authors' knowledge, no joint angle recovery method suitable for arbitrary motion has yet been tested on rehabilitation patients.

This paper evaluates the performance of a joint estimation algorithm that utilizes strap-on IMU sensors in a clinical rehabilitation setting. The data collected from the IMU sensors is processed in a Kalman filter framework to estimate the joint angles of the patient performing arbitrary 3D movement. The approach is validated using data obtained during post-surgery rehabilitation for lower body total joint replacement patients.

II. JOINT ANGLE RECOVERY ALGORITHM

Movement data is collected from the patients via IMUs attached to the limb undergoing rehabilitation. The data is combined with a kinematic model in an extended Kalman filter (EKF) to estimate the patient's joint angles [5]. The algorithm allows the patient's joint angles to be determined on-line, regardless of the patient's posture or movement speed. The EKF was chosen for its mathematical simplicity. Initial explorations into more general algorithms such as the unscented Kalman filter or the particle filter yielded no noticeable improvement in computational accuracy, or were deemed too computationally expensive for the application.

J. F. Lin and D. Kulić are with the Department of Electrical and Computer Engineering, University of Waterloo, Waterloo, ON, N2L 3G1, Canada (email: jf2lin@uwaterloo.ca; dkulic@ece.uwaterloo.ca)

A. Forward kinematics

The human leg is modeled as an articulated chain of rigid bodies (leg limbs), connected by a sequence of joints (hip, ankle and knee). The hip is modeled as a set of 3 co-located revolute joints, resulting in 3 degrees of freedom (DOF) at the hip joint, while the knee is modeled as a 2 DOF joint. A reference frame (denoted as the i^{th} frame) is attached to each DOF (denoted as the $i-1^{th}$ joint) according to the Denavit-Hartenberg convention [13].

The forward kinematics of any articulated chain is computed by successively applying frame transformations with rotational matrices $R_{i-1,i}$ [14]. Given the angular velocity of the preceding frame ω_{i-1}^{i-1}, and the joint velocity $\dot{q}_i$, generated by joint i, the angular velocity ω_i^i of the next frame can be calculated. The angular acceleration α_i^i can be obtained by differentiating ω_i^i:

$$\omega_i^i = R_{i-1,i}^T \omega_{i-1}^{i-1} + R_{i-1,i}^T \dot{q}_i \tag{1}$$

$$\alpha_i^i = R_{i-1,i}^T \alpha_{i-1}^{i-1} + R_{i-1,i}^T \ddot{q}_i + \omega_i \times (R_{i-1,i}^T \dot{q}_i) \tag{2}$$

The linear velocity of the current frame $\dot{x}_i$ is obtained by computing the cross-product of the angular velocity and displacement vector from the center of the current frame to the center of the previous frame r_i. Differentiation is carried out again to obtain the linear acceleration $\ddot{x}_i$:

$$\dot{x}_i = R_{i-1,i}^T \dot{x}_{i-1} + \omega_i^i \times r_i \tag{3}$$

$$\ddot{x}_{e,i} = R_{i-1,i}^T \ddot{x}_{e,i-1} + \alpha_i^i \times r_i + w_i^i \times (w_i^i \times r_i) + R_{0,i} g \tag{4}$$

In (4), an extra $R_{0,i}g$ term is added to model gravity and to rotate it into the local frame.

B. Extended Kalman filter

The EKF [15] is a sensor fusion technique that estimates the system state from a state evolution and measurement observation model. The filter first updates the state estimate based on the state evolution model, and then corrects the estimate based on the measurement variables and the measurement observation model. The state estimate s_t and observation update z_t are defined as:

$$s_t = f(s_{t-1}) + w_t \tag{5}$$

$$z_t = h(s_t) + v_t \tag{6}$$

Here, the joint angles, velocities and accelerations for each DOF are used as the state variables, while the accelerations and angular velocities obtained from the accelerometer and gyroscope are used as the measurement variables. Kinematic equations assuming constant acceleration are used as the state model $f(s_{t-1})$ in Equation 5:

$$q_t = q_{t-1} + \dot{q}_{t-1} t + \ddot{q}_{t-1} t^2/2 \tag{7}$$

$$\dot{q}_t = \dot{q}_{t-1} + \ddot{q}_{t-1} t \tag{8}$$

$$\ddot{q}_t = \ddot{q}_{t-1} \tag{9}$$

The observation model $h(s_t)$ is defined by Equations 1 and 4, where $\ddot{x}_{e,i}$ and ω_i^i correspond to the local accelerometer and gyroscope measurements [5].

TABLE I

OBSERVED EXERCISE MOTIONS, WITH THEIR INITIAL POSTURE (POSTURE), ALONG WITH THE NUMBER OF PATIENTS (COUNT) AND PERCENTAGE OF TIME (TOTAL) SPENT PERFORMING ANY GIVEN MOTION. ALL VALUES IN [%].

	Name [18]	Posture	Count	Total
AR.ST	Heel/toe raise	Standing	85.7	5.9
BK.SU	Bridging	Supine	42.9	1.8
HA.ST	Side leg lift	Standing	57.1	3.8
HA.SU	Leg slides to side	Supine	57.1	3.9
HE.ST	Leg straight back	Standing	71.4	3.2
HF.ST	Leg straight forward[2]	Standing	42.9	2.7
HF.SU	Leg straight up[2]	Supine	42.9	2.1
KE.SI	Knee straightening	Sitting	71.4	10.2
KE.SU	Heel raise	Supine	100.0	14.3
KF.SI	Knee bends	Sitting	14.3	0.6
KF.ST	Heel lift	Standing	85.7	7.3
KF.SU	Heel pushes	Supine	57.1	5.5
KH.ST	Knee lift	Standing	71.4	6.8
KH.SU	Knee/hip bend	Supine	100.0	25.1
LU.ST	Lunges[2]	Standing	28.6	1.9
SQ.ST	Squats[2]	Standing	71.4	4.8

[1] Motion not analyzed in this paper.

To perform optimal estimation, the EKF requires accurate process (w_t) and measurement (v_t) noise models to account for factors such as unmodeled terms in the state or observation equations, or sensor noise in the measurement. These factors depend on a variety of different conditions, such as movement velocity or ambient temperature, and need to be adapted during the state recovery process to produce a more accurate estimation. A symptom of poor modeling is state estimate divergence. When divergence is observed from poorly conditioned EKF intermediate matrices, the state estimate can be reset and the noise covariances is increased, as a method to automatically tune the noise parameters. A potential field [16] is also implemented to enforce anthropometric joint limits, to reduce the impact of drift [5].

III. EXPERIMENTS AND RESULTS

The IMU data for 7 lower body total joint replacement (TJR) in-patients (2 M, 5 F) were collected at the Toronto Rehabilitation Institute. The patients were tracked from the first day of admission until discharge, with the average patient's treatment lasting 5.7 days. The patients engaged in rehabilitation every day during the course of their treatment, and data was collected during each weekday session, for roughly an hour per session. The patients were also instructed to perform exercises outside of these sessions, but these unsupervised exercises were not captured. During the rehabilitation sessions, three SHIMMER [17] IMUs were attached by Velcro straps to the hip, knee and ankle of the patient. The patient was asked to verify that the straps were not uncomfortable or hampered their movement before the data collection began. The average age of the participants was 71.9 $\pm$ 9 years old. The experiment was approved by the University of Waterloo Research Ethics Board and the University Health Network Research Ethics Board, and signed consent was obtained from all participants.

The motions performed by the various patients were the exercises prescribed by the physiotherapist, based on their assessment of the patient's progress. TJR rehabilitation tends to include a regular set of exercises, such as heel raises, hip and knee bends, knee straightening and knee lifts [18]. However, a patient's exercise regime may change based on the nature of their operation and recovery rate, so certain patients might not perform certain exercises, or may have additional exercises added. The data examined for this paper accounts for over 90% of the exercises observed, excluding bridge and heel raises. These two types of motions were excluded as they include ankle movement, which cannot be recovered with the sensor placement used in this dataset (due to the lack of sensor at the foot). The exercises collected, along with the percentage of time patients spent performing each exercise, are shown in Table I. 14 different types of exercises were analyzed, for a total of 477 minutes of data.

All analysis was performed with MATLAB 7.12. The EKF functions were implemented with the ReBEL MATLAB Toolbox [19]. The initial noise covariance profile used to describe w_t and v_t was tuned for a single subject by minimizing the error between the observation data and the forward kinematic reconstruction from recovered joint angle, velocity and acceleration. This noise profile was applied to the remaining 6 participants.

Unlike [5], a motion capture system was not available at the rehabilitation clinic. Values derived from anthropometric tables [20] were used for the link lengths for all participants. This also means that no motion capture ground truth data was available to verify the accuracy of the state estimates. Two alternative measures were examined instead to analyze the accuracy of the algorithm: 1) sensor error, where the root-mean-square (RMS) error between the collected accelerometer and gyroscope data and the forward kinematic reconstruction from the state estimate is calculated, 2) key pose error, where key stationary poses in the movement are identified, and the joint angle RMS error between the first key pose and subsequent key poses in the movement sequence is calculated.

The ground truth data for the sensor error is calculated by processing the IMU data with a dual-pass Butterworth filter to reduce high frequency sensor noise. These error results can be seen in Table II. Table II shows good reconstruction results. For the accelerometer, the largest contributor to the acceleration signal is gravity, at 9.81 m/s^2. If the joint recovery is poor, then the acceleration reconstruction would show errors comparable to that of gravity. The EKF algorithm achieves accelerometer reconstruction errors less than 5% of gravity. For the gyroscope, the data can be compared against a joint recovery system that relies on only accelerometer incline to obtain joint angle. Inclinometry systems can only determine tilt and heading, and thus are not able to estimate movements that involve hip abduction movement. The proposed system, with a gyroscope RMS error of 0.09 rad/s, outperforms the inclinometer, with a gyroscope RMS error of 0.11 rad/s.

The IMU RMS errors reported above do not capture drift error. For example, if drift occurs in the transverse plane, due to abduction-adduction motion, the accelerometer error would not increase as the biggest contribution to acceleration is gravity, and gravity does not impact the abduction motion for sagittal movements. The second assessment tool, based on key poses, is employed to capture potential drift error. To evaluate the magnitude of the position error, the cyclic nature of the rehabilitation movement is utilized, where the patient returns to an initial pose after each repetition. If drift error is small, it can be expected that following the end of each repetition, the joint angle position is approximately the same. The pose at the start of each repetition is termed the *key pose*. An error metric can be generated by designating the first key pose as the baseline and comparing subsequent key poses against it. However, if the patient does not return to their initial joint configuration at the beginning of each motion, this offset would be incorrectly attributed as error.

TABLE II

ACCELEROMETER AND GYROSCOPE RMS ERRORS BY MOTION TYPE. ERROR REPORTED FOR THE UPPER LINK (U), LOWER LINK (L), AND OVERALL AVERAGE (AV).

	Accelerometer $[m/s^2]$			Gyroscope $[rad/s]$		
	U	L	AV	U	L	AV
HA.ST	0.40	0.48	0.44	0.14	0.15	0.14
HA.SU	0.46	0.50	0.48	0.09	0.09	0.09
HE.ST	0.41	0.50	0.45	0.11	0.13	0.12
HF.ST	0.49	0.52	0.50	0.13	0.14	0.14
HF.SU	0.33	0.34	0.34	0.04	0.08	0.06
KE.SI	0.43	0.61	0.52	0.06	0.16	0.11
KE.SU	0.34	0.32	0.33	0.03	0.06	0.05
KF.SI	0.26	0.21	0.24	0.03	0.06	0.04
KF.ST	0.41	0.58	0.49	0.12	0.20	0.16
KF.SU	0.35	0.36	0.36	0.05	0.08	0.06
KH.ST	0.52	0.49	0.50	0.13	0.14	0.14
KH.SU	0.43	0.36	0.39	0.07	0.07	0.07
LU.ST	0.20	0.30	0.25	0.05	0.04	0.04
SQ.ST	0.27	0.32	0.29	0.09	0.09	0.09
AV	0.38	0.42	0.40	0.08	0.11	0.09

To automatically identify key poses in the continuous time series data, the recovered joint angles are filtered and differentiated to obtain joint velocity. The joint angle with the largest velocity is selected to be the significant DOF. At the key pose, a zero-velocity crossing (ZVC) is observed, where the velocity is zero, while the velocity prior and subsequent to the key pose differs in sign, as shown in Fig. 1. This way, key poses can be identified consistently and automatically.

The first ZVC that is in front of a velocity peak that is within 70% of the largest velocity value in the entire motion sequence is selected to be the baseline key pose. Subsequent ZVC points that precede large peaks are identified; these points are assumed to be the start of each repetition. Large peaks are selected to prevent small movements from triggering the comparison process. Table III reports the key pose joint angle errors for each motion type.

The errors reported here are comparable to the results of the algorithm used with healthy participants [5]. For the healthy subjects, an angular RMS error of 0.13 rad and 0.10 rad was reported, for upper and lower joints respectively.

TABLE III

JOINT ANGLE RMS ERROR [rad] AT EACH KEY POSE BY MOTION TYPE. ERROR REPORTED FOR EXTENSION-FLEXION (EF), ABDUCTION-ADDUCTION (AA), INTERNAL ROTATION (IR), UPPER LINK (U), LOWER LINK (L) AND OVERALL AVERAGE (AV).

	Upper Leg			Lower Leg		Average		
	EF	IR	AA	EF	IR	U	L	AV
HA.ST	0.10	0.51	0.15	0.05	0.20	0.25	0.13	0.20
HA.SU	0.06	0.06	0.35	0.05	0.06	0.16	0.05	0.12
HE.ST	0.08	0.14	0.07	0.08	0.18	0.10	0.13	0.11
HF.ST	0.08	0.19	0.06	0.07	0.20	0.11	0.13	0.12
HF.SU	0.02	0.07	0.14	0.04	0.04	0.08	0.04	0.06
KE.SI	0.05	0.11	0.17	0.14	0.25	0.11	0.20	0.14
KE.SU	0.05	0.09	0.18	0.05	0.06	0.11	0.06	0.09
KF.SI	0.04	0.16	0.18	0.08	0.20	0.13	0.14	0.13
KF.ST	0.10	0.17	0.08	0.15	0.18	0.12	0.16	0.14
KF.SU	0.04	0.09	0.16	0.05	0.07	0.09	0.06	0.08
KH.ST	0.14	0.22	0.09	0.12	0.33	0.15	0.23	0.18
KH.SU	0.07	0.09	0.17	0.11	0.10	0.11	0.10	0.11
LU.ST	0.10	0.15	0.05	0.10	0.11	0.10	0.11	0.10
SQ.ST	0.08	0.19	0.06	0.09	0.18	0.11	0.14	0.12
AV	0.07	0.16	0.14	0.09	0.15	0.12	0.12	0.12

With the patient population, the proposed algorithm reports 0.12 rad and 0.12 rad for the same joints. An examination of Table III shows that, similar to the healthy subjects [5], the error tends to be smaller in the sagittal plane, suggesting that drift remains a concern for both datasets. These results demonstrate promise for use in a clinical setting. However, a direct comparison between this paper and [5] cannot be made because the errors reported in [5] was made by comparing the joint angle estimation to motion capture data at every measurement time step, whereas this paper compares key poses to the baseline key pose.

IV. CONCLUSIONS AND FUTURE WORK

A system for joint angle recovery from ambulatory sensors was validated in a clinical setting with joint replacement patients undergoing physiotherapy. The approach is based on an EKF framework incorporating kinematic constraints by modeling the patient limb as a kinematic chain. The proposed algorithm achieves an accelerometer RMS error of 0.40 m/s^2 and a gyroscope RMS error 0.09 rad/s. An examination of key poses throughout the exercises showed an overall angular RMS error of 0.12 rad with respect to the initial key pose.

For future work, data from additional patients and injury types will be collected. Different types of exercises, particularly functional exercises such as walking will also be examined. More sophisticated state models beyond the constant-acceleration model will also be considered.

V. ACKNOWLEDGMENT

The authors would like to thank the physiotherapists and patients of the Toronto Rehabilitation Institute for providing the time and data utilized for this work.

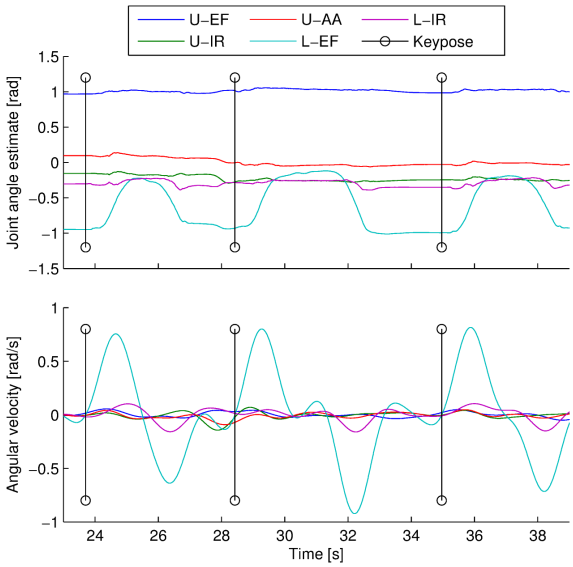

Fig. 1. Joint angles (top) and angular velocity (bottom) of a subject performing knee straightening exercises. Black vertical lines denote key pose positions.

REFERENCES

[1] H. Zhou *et al.*, "Use of multiple wearable inertial sensors in upper limb motion tracking," *Med. Eng. Phys.*, vol. 30, pp. 123–133, 2008.

[2] J. Bergmann *et al.*, "A portable system for collecting anatomical joint angles during stair ascent: a comparison with an optical tracking device," *Dyn. Med.*, vol. 8, pp. 1–7, 2009.

[3] M. C. Boonstra *et al.*, "The accuracy of measuring the kinematics of rising from a chair with accelerometers and gyroscopes," *J. Biomech.*, vol. 39, pp. 354–358, 2006.

[4] H. Luinge and P. Veltink, "Measuring orientation of human body segments using miniature gyroscopes and accelerometers," *Med. Biol. Eng. Comput.*, vol. 43, pp. 273–282, 2005.

[5] J. F. S. Lin and D. Kulić, "Human pose recovery using wireless inertial measurement units," *Physiol. Meas.*, vol. 33, pp. 2099–2115, 2012.

[6] H. Krebs *et al.*, "Rehabilitation robotics: pilot trial of a spatial extension for MIT-Manus," *J. Neuroengineering. Rehabil.*, vol. 1, pp. 5–20, 2004.

[7] Y. Sankai, "Hal: Hybrid assistive limb based on cybernics," in *Robotics Research*. Springer Berlin/Heidelberg, 2011, vol. 66, pp. 25–34.

[8] E. Strickland, "Good-bye, wheelchair," *IEEE Spectrum*, vol. 49, pp. 30–32, 2012.

[9] S. Hong *et al.*, "An effective method of gait stability analysis using inertial sensors," in *MICAI 2006: Advances in Artificial Intelligence*. Springer Berlin/Heidelberg, 2006, vol. 4293, pp. 1220–1228.

[10] H. Simila *et al.*, "Human balance estimation using a wireless 3D acceleration sensor network," in *Proc. IEEE Int. Conf. Eng. Med. Biol. Soc.*, 2006, pp. 1493–1496.

[11] A. Salarian *et al.*, "iTUG, a sensitive and reliable measure of mobility," *IEEE Trans. Neural Syst. Rehabil. Eng.*, vol. 18, pp. 303–310, 2010.

[12] F. Cavallo *et al.*, "A first step toward a pervasive and smart ZigBee sensor system for assistance and rehabilitation," in *Proc. IEEE Int. Conf. Rehabilitation Robotics*, 2009, pp. 632–637.

[13] J. J. J. Uicker *et al.*, "An iterative method for the displacement analysis of spatial mechanisms," *J. Appl. Mech.*, vol. 31, pp. 309–314, 1964.

[14] M. W. Spong *et al.*, *Robot Modeling and Control*, C. Shultz, Ed. John Wiley and Sons, Inc., 2006.

[15] G. Welch and G. Bishop, "An introduction to Kalman filters," University of North Carolina at Chapel Hill, Tech. Rep., 2006.

[16] O. Khatib, "Real-time obstacle avoidance for manipulators and mobile robots," in *Proc. IEEE Int. Conf. Robot. Autom.*, 1985, pp. 500–505.

[17] A. Burns *et al.*, "Shimmer: A wireless sensor platform for noninvasive biomedical research," *IEEE Sensors J.*, vol. 10, pp. 1527–1534, 2010.

[18] Toronto Rehabilitation Institute, "Hip and knee exercises."

[19] E. A. Wan and A. T. Nelson, *Kalman Filtering and Neural Networks*. John Wiley and Sons, Inc., 2001, ch. Dual EKF Methods, pp. 123–173.

[20] C. C. Norkin and D. J. White, *Measurement of Joint Motion: A Guide to Goniometry, 4th Edition*. F. A. Davis Company, 2009.